Characterization of Photon Pair Source for Entangled Two-Photon Absorption Experiments

JUAN CAMILO REALES CRESPO[1], PROF. MAYERLIN NUÑEZ PORTELA[2], AND MICHAEL STIVEN CARACAS[3]

[1] *Department of Physics, Quantum optics laboratory, Universidad de los Andes, 2024 Bogotá D.C, Colombia*
[*] *j.reales@uniandes.edu.co, m.nunez@uniandes.edu.co, ms.caracas@uniandes.edu.co*

Compiled June 11, 2024

In this study, we utilize a Beta Barium Borate (BBO) type I nonlinear crystal to produce pairs of entangled photons. These pairs, referred to as signal and idler photons, have distinctive entanglement properties that are foundational for technologies like quantum cryptography and quantum teleportation. The photons are generated through a process called Spontaneous Parametric Down-Conversion (SPDC), which occurs when a pump laser beam passes through a nonlinear medium. This process is governed by the conservation of momentum and energy, resulting in specific phase-matching conditions that dictate the spatial and frequency correlations of the photon pairs. The objective of this project is to characterize these entangled photon pairs by examining their temporal correlation based on a coincidence detection system.

1. INTRODUCTION

Photon pair sources, particularly those based on spontaneous parametric down-conversion (SPDC), have become indispensable tools in quantum optics and quantum information science. The ability to generate entangled photon pairs has paved the way for numerous groundbreaking experiments and applications, including quantum cryptography, quantum computing, and advanced spectroscopy techniques. In this article, we focus on the characterization of a photon pair source tailored for entangled two-photon absorption (ETPA) experiments, a field that promises enhanced sensitivity and specificity in molecular spectroscopy.

ETPA leverages the unique properties of entangled photons to probe multiphoton transitions in molecules with greater precision than classical two-photon absorption (TPA) methods. Unlike classical TPA, where uncorrelated photon pairs drive two-photon transitions, ETPA exploits the quantum correlations between entangled photon pairs, leading to new possibilities in studying nonlinear optical processes at lower photon fluxes.

Our work aims to characterize a photon pair source optimized for ETPA experiments comprehensively. This includes a detailed examination of the SPDC process, the experimental setup for generating and detecting entangled photon pairs, and the specific configurations used to achieve high detection efficiency. Additionally, we present a case study involving rhodamine B molecules, demonstrating the practical application of the characterized photon pair source in measuring ETPA cross-sections.

The structure of this article is as follows: We begin with the theoretical foundation of SPDC and its implementation using a BBO crystal. This is followed by the experimental setup description, including the optical alignment and detection systems. We then present the results of our photon-pair source characterization and discuss its implications for ETPA measurements. Finally, we conclude with insights into the potential advancements in multiphoton spectroscopy enabled by entangled photon pairs [1].

2. THEORETICAL FOUNDATION

A. Spontaneous Parametric Down-Conversion (SPDC)

SPDC is a process where a nonlinear crystal interacts with a laser beam, producing correlated photon pairs called signal and idler photons (Figure 1).

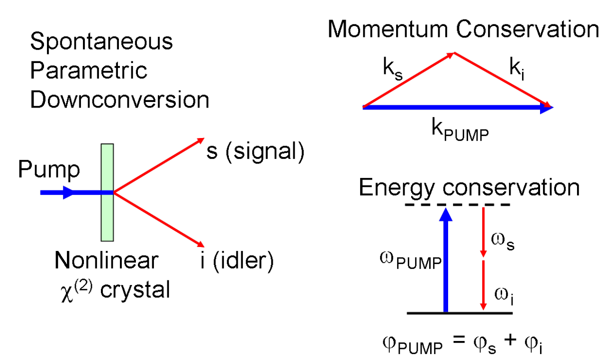

Fig. 1. Schematic of SPDC process.

This interaction is described by the second-order magnetic susceptibility tensor $\chi^{(2)}_{ijk}$ [2]. When the crystal interacts with the laser field, the interaction Hamiltonian can be expressed as:

$$\mathcal{H}_{\text{int}} = \varepsilon_0 \int_v \chi^{(2)}_{ijk} E_i E_j E_k d^3r$$

Using first-order perturbation theory, the photon pair state $|\psi\rangle$ can be derived as:

$$|\psi\rangle = -\frac{i}{\hbar} \int H_{\text{int}}(t)|0\rangle$$

The phase-matching conditions, $\omega_p = \omega_s + \omega_i$ and $\mathbf{k}_p = \mathbf{k}_s + \mathbf{k}_i$, ensure energy and momentum conservation. SPDC can produce photons with the same polarization (type-I SPDC) or orthogonal polarizations (type-II SPDC). Non-collinear SPDC occurs when the photon pairs' directions differ from the pump source (Figure 2).

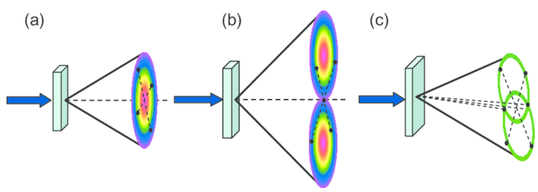

Fig. 2. Three different types of parametric down-conversion schemes: (a) type-I phase-matching; (b) collinear degenerate type-II phase-matching, with two cones overlapping along the pump direction; (c) non-collinear degenerate type-II phase-matching—the cones intersect along two symmetric directions.

B. Entangled Two-Photon Absorption (ETPA)

Entangled Two-Photon Absorption (ETPA) is a quantum process in which two entangled photons are simultaneously absorbed by a material, typically leading to higher efficiency and unique applications compared to traditional Two-Photon Absorption (TPA) [3].

In TPA, the absorption of two independent photons occurs simultaneously, requiring high photon flux and often resulting in low efficiency. ETPA, on the other hand, leverages the quantum entanglement of photon pairs, enhancing the probability of simultaneous absorption. This makes ETPA more efficient even at lower photon fluxes, which is advantageous for applications in spectroscopy, imaging, and quantum information processing.

The two-photon absorption rate R of a sample interacting with photon pairs can be expressed as a function of the incident photon flux, Φ [4]:

$$\mathcal{R}(\phi) = \sigma_e^{(2)}\phi + \sigma^{(2)}\phi^2 \quad \textbf{(1)}$$

The factor $\sigma^{(2)}$ represents the effective cross-section for classical TPA with coherent light, while $\sigma_e^{(2)}$ denotes the effective cross-section for ETPA. In the low photon flux regime, $R(\Phi)$ is linear, and entangled photon pairs drive the two-photon transition in the sample [5]. When excitation is performed with uncorrelated light sources, such as laser light, only the quadratic term in $R(\Phi)$ is present.

A typical experiment to measure the absorption signal using a coincidence detection system is illustrated in Figure 3.

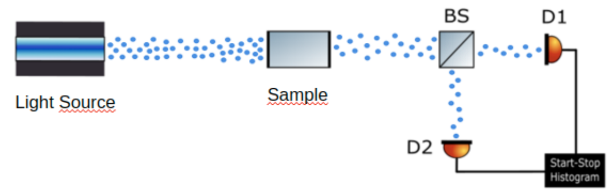

Fig. 3. The schematic of a TPA experiment using a coincidence detection system. Light from the source hits the sample, and the transmitted light reaches a beam splitter (BS). The light in both arms then reaches detectors D1 and D2. Image adapted from [6]

From this experiment, the coincidence count rate $\mathcal{R}_c$ between the two detectors D1 and D2 can be deduced as:

$$\mathcal{R}_c \sim \int_0^{\tau_{coin}} d\tau S(\tau - t_0) G^{(2)}(\tau), \quad \textbf{(2)}$$

where $G^{(2)}(\tau)$ denotes the second-order temporal correlation function, and $S(\tau - t_0)$ is the coincidence window function centered at t_0 with a width τ_{coin} [7].

To quantify single-photon losses (SPL) on coincidence rates with entangled photons, we consider two scenarios: attenuating the pump beam before the nonlinear crystal and attenuating the photon pairs after the crystal [8]. Attenuators are characterized by η_{att}, representing the transmission probability of photons.

Assuming a photon flux Φ_{pump} and losses ϵ_1 and ϵ_2 in the paths to detectors D1 and D2, the coincidence rate R_c is given by $R_c = \epsilon_1\epsilon_2\eta_{SPDC}\Phi_{pump}$, where η_{SPDC} is the SPDC efficiency. For pump beam filtering:

$$R_c = \epsilon_1\epsilon_2\eta_{SPDC}\eta_{att}\Phi_{pump} \quad \textbf{(3)}$$

For filtering the photon pairs:

$$R_c = \epsilon_1\epsilon_2\eta_{SPDC}\eta_{att}^2\Phi_{pump} \quad \textbf{(4)}$$

Here, η_{att} is squared, considering both signal and idler photon transmission probabilities.

3. EXPERIMENTAL SETUP

Four key pillars are implemented to characterize the entangled photon pair source: characterization of the pump beam, analysis of the spatial profile of photon pairs, a coincidence detection system, and quantification of the $G^2(\tau)$ using a signal detection mechanism for ETPA.

A. Pumping Laser Characterization

First, an extended-cavity diode laser (NVD4916) operating at 412 nm in a Littrow configuration is used to generate the pump beam. Secondly, to understand the beam behavior along the optical path, a beam profiler (BeamMaster USB BM-7 Si-enhanced, Coherent) was used. This device provides the spatial intensity distribution of the incident light, allowing the determination of the beam waist ($\mathcal{W}$) and Rayleigh range (Z_R). Measurements were taken at various distances from the light source, with the zero point set at the dichroic mirror (MD). From the data, as shown in Figure 4, it was found that:

$$\begin{aligned} \mathcal{W}_{0x} &= (73 \pm 1)\mu m \\ Z_{Rx} &= (4.2 \pm 0.1)cm \end{aligned} \tag{5}$$

$$\begin{aligned} \mathcal{W}_{0y} &= (77 \pm 1)\mu m \\ Z_{Ry} &= (4.5 \pm 0.1)cm \end{aligned} \tag{6}$$

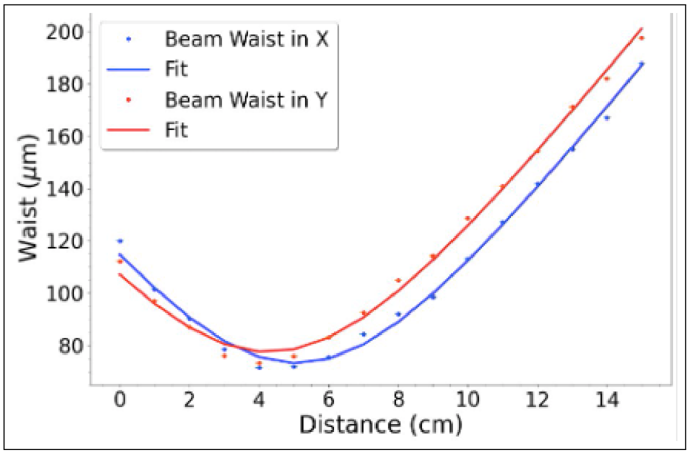

Fig. 4. Laser waist taken with the BeamMaster as a function of the distance taken from the MD.

To generate correlated photon pairs, a birefringent nonlinear crystal is used. Specifically, a type I negative uniaxial BBO crystal with dimensions of 6 mm × 6 mm × 1 mm is employed. The crystal is mounted with degrees of freedom to produce either collinear or non-collinear SPDC. The transition between collinear and non-collinear configurations depends on the orientation of the crystal's optical axis relative to the pump beam's propagation direction.

The light must be focused on the crystal for the BBO crystal to generate highly correlated photon pairs (maximizing the number of pairs per incident photon). To achieve this focus, A focal length lens $L_1 = 4.5$ mm collimates the beam along the entire length of the experimental setup. The Gaussian profile generated by this type of beam can be seen in Figure 5.

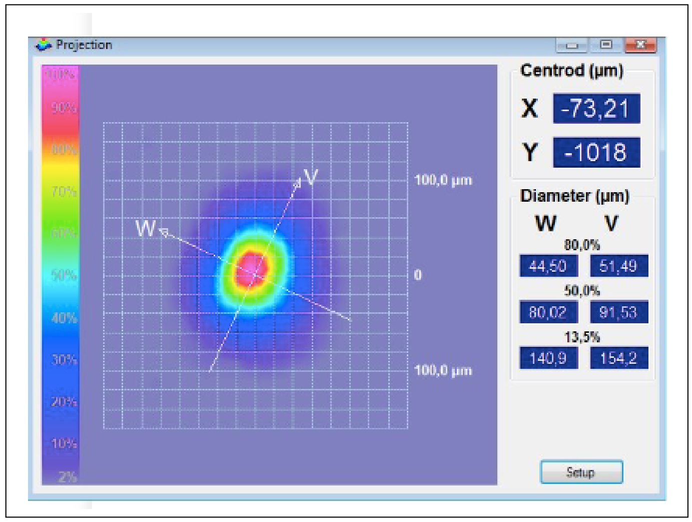

Fig. 5. Spatial distribution of the pump beam intensity - transverse section. Post-lens waist focusing on the BBO using BeamMaster with lenses $L_1 = 4.5$mm and $L_2 = 200$ mm. The Gaussian beam diameter is characterized by the width of its spatial distribution, where measurements in micrometers correspond to values given at 13.5 % of intensity (140.9 μm horizontally, W, and 154.2 μm vertically, V).

B. Photon Pair Spatial Profile

Subsequently, by positioning the crystal within the Z_R, the rings generated by the BBO were observed using a CCD camera (STF-402-M-C2, SBIG) placed after the crystal. Four high-pass filters were placed at the camera entrance to block blue light. Utilizing the degrees of freedom provided by the crystal mount, the rings were adjusted from a noncollinear to a collinear configuration, as shown in Figure 7. Then, through a telescope system, the pumping beam is focused on the BBO crystal, as shown in figure 6, achieving a beam waist of 64 μm.

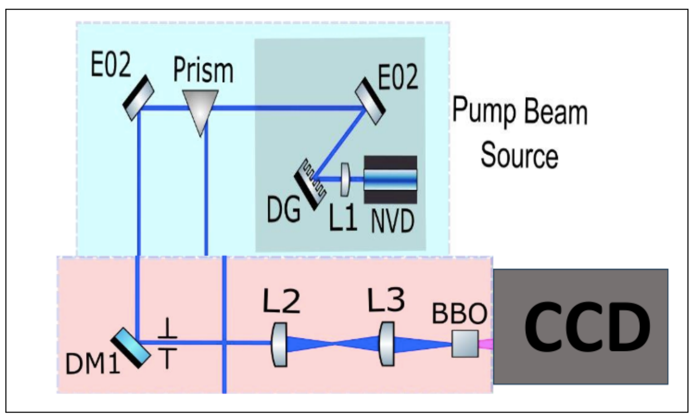

Fig. 6. Assembly of the focusing telescope and camera system with which SPDC rings are observed. The telescope system comprises two lenses L2 and L3, with 200mm and 70mm focal lengths respectively.

We are particularly interested in a type I collinear SPDC configuration for our experiment due to its significant advantages. In type I collinear SPDC, both generated photons have the same polarization and propagate along the same direction as the pump beam. This simplifies the alignment and detection process, enhancing the efficiency and reliability of the photon pair generation. Additionally, the collinear configuration maximizes the overlap between the signal and idler photons, leading to higher coincidence counts and improved signal-to-noise ratio, which is crucial for accurate measurements in our experimental setup.

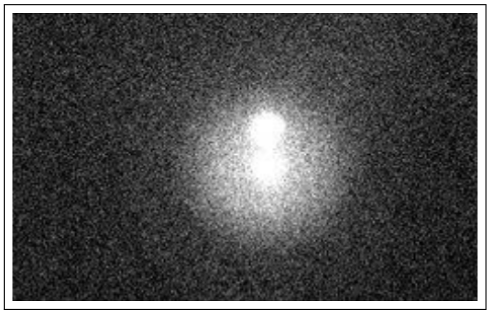

(a) Ring found with collinear SPDC-I configuration.

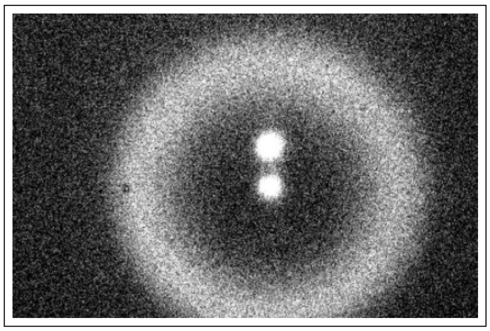

(b) Ring found with non-collinear SPDC-I configuration.

Fig. 7. SPDC rings produced by the BBO type I crystal, images taken with a CCD camera.

C. Coincidence Detection

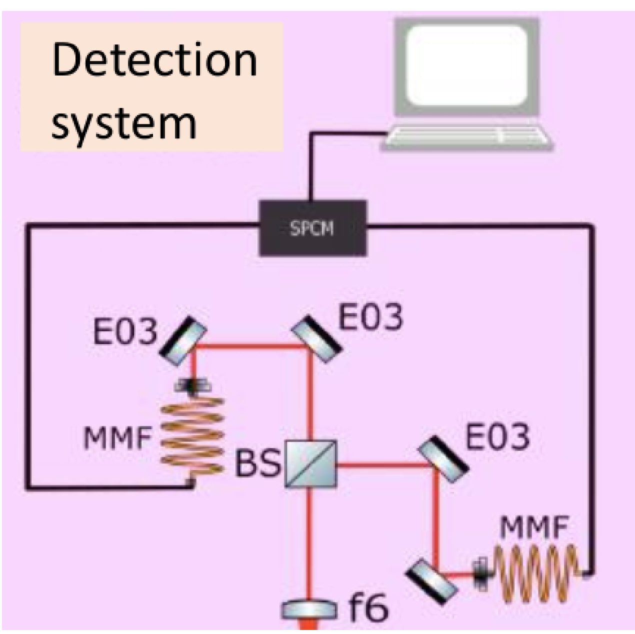

Fig. 8. HBT and coincidence detection system.

The coincidence detection system is based on a Hanbury Brown and Twiss interferometer (HBT). This setup includes a 50 : 50beam splitter (BS) and four mirrors (E03) that direct the photons to two multi-mode fiber couplers (MMF). These fibers are connected to single-photon counting modules (SPCM), and the temporal correlation between the photon pairs is analyzed using a time-to-digital converter.

D. ETPA signal in Rhodamine B (RhB)

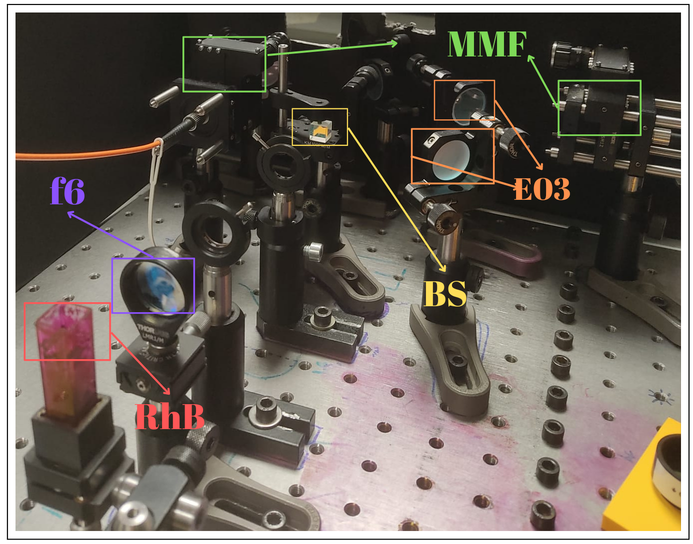

Fig. 9. Set-up for ETPA detection in RhB.

To demonstrate the utility of an entangled photon pair source in experiments involving multiphoton transitions, we conducted an example measurement of ETPA in rhodamine B molecules. Rhodamine B (RhB) is commonly used for entangled two-photon absorption (ETPA) experiments due to its strong two-photon absorption (TPA) characteristics, making it an ideal candidate for studying nonlinear optical processes [9].

To study the ETPA cross-section in RhB molecules, we will measure the coincidence rate for three scenarios: without a sample, with only the solvent (methanol), and with a RhB solution in methanol at a concentration of 50 mM. Measurements with only methanol will help quantify the effects of single photon loss (SPL). The goal is also to measure the coincidence rate as a function of the pump beam power. This will involve filtering the beam using neutral density filters with optical densities ND = 0.0 to 1.0. Filtering will be done in two ways: filtering the pump beam (placing the filters before the BBO crystal) and filtering the photon pairs (placing the filters after the BBO crystal). This approach aims to quantify the effects of SPL again. Then, we obtained:

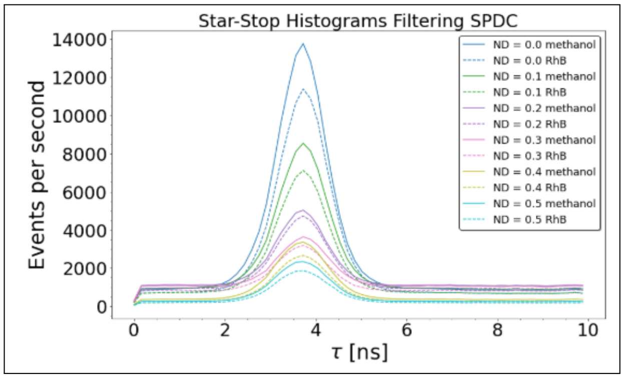

(a) Start-stop histogram filtering SPDC.

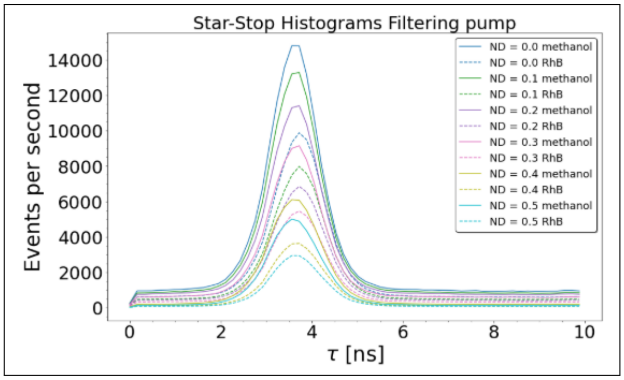

(b) Start-stop histogram filtering pump.

Fig. 10. Start-stop histograms are generated from the coincidence counting rate using the SPCM. These histograms are produced for various pump beam power levels, and filtered using neutral density (ND) filters. The histograms illustrate three scenarios: no sample present, the sample is methanol (solvent), and the sample is a Rhodamine B solution.

4. RESULTS AND DISCUSSIONS

The start-stop histograms in Figure 10 can be used to identify genuine coincidence events. This is done by integrating the histograms within a specific time window that corresponds to the chosen temporal bin size for the measurements, using equation (2). In this case, the time window is 1.76 ns. The real coincidence events can be determined by locating the peak in the histogram and integrating around that maximum, over the 1.76 ns window. Additionally, the histograms are integrated outside of this time window to capture the accidental coincidences - those that do not correspond to the arrival of photon pairs at the detectors. After obtaining the real and accidental coincidence counts, these values are then plotted against the individual photon counts, or singles, recorded by one of the detectors (D_1 or D_2). As shown in the figure 11.

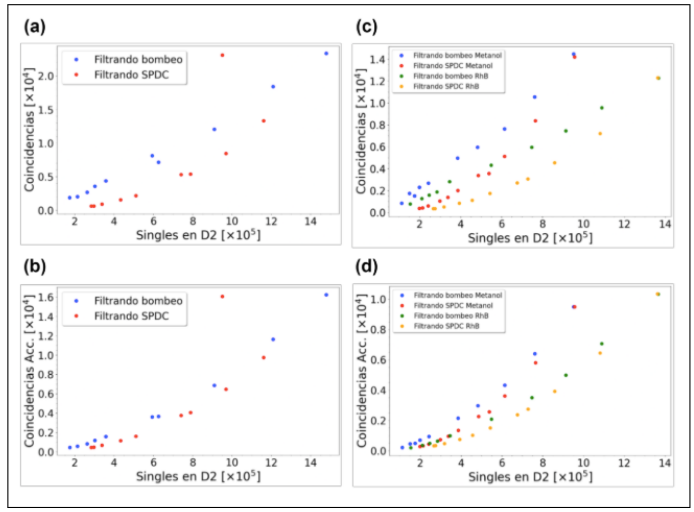

Fig. 11. Graphical Representation of Actual and Accidental Coincidences Relative to Singles in Detector D2 a) and b) represent the case where no sample is present. c) and d) correspond to the case where the sample is Methanol and a Rhodamine B solution.

The graphs in Figure 11 illustrate the linear relationship between the coincidence counts and the filtered pump beam, as predicted by Equation (3). In contrast, the coincidence counts plotted against the singles show a quadratic behavior when the photon pairs are filtered, in accordance with Equation (4). Regarding the accidental coincidences, the data reveals a quadratic dependence on the single counts, regardless of the filtering scheme employed.

The results indicate a clear decrease in the number of coincidences when Rhodamine B is present, as shown in the graphs in figure 11. This reduction is attributed to entangled two-photon absorption (ETPA) by RhB molecules, which efficiently absorb the entangled photon pairs. The presence of RhB results in fewer detected photon pairs, confirming ETPA's role in the observed decrease in coincidences.

5. CONCLUSSIONS

In conclusion, this study has provided a comprehensive characterization of a photon pair source optimized for entangled two-photon absorption (ETPA) experiments. The detailed analysis of the spontaneous parametric down-conversion (SPDC) process and the experimental setup has demonstrated the ability to generate highly correlated photon pairs with favorable properties for ETPA measurements. The case study involving rhodamine B molecules showcases the practical application of this photon pair source in measuring ETPA cross-sections. Looking ahead, the potential to apply this technique to study nonlinear optical processes in cesium atoms holds promise for advancements in quantum optics and spectroscopy. However, typical challenges in these types of experiments, such as low photon fluxes and the need for efficient detection systems, will need to be addressed in future work to further improve the sensitivity and reliability of ETPA-based measurements.

REFERENCES

1. Gisin, N., Ribordy, G., Tittel, W. & Zbinden, H. Quantum cryptography. *Rev. modern physics* **74,** 145 (2002).

2. Couteau, C. Spontaneous parametric down-conversion. *Contemp. Phys.* **59,** 291–304 (2018).

3. Tabakaev, D. *et al.* Spatial properties of entangled two-photon absorption. *Phys. Rev. Lett.* **129,** 183601 (2022).

4. Fei, H.-B., Jost, B. M., Popescu, S., Saleh, B. E. & Teich, M. C. Entanglement-induced two-photon transparency. *Phys. review letters* **78,** 1679 (1997).

5. Schlawin, F., Dorfman, K. E. & Mukamel, S. Entangled two-photon absorption spectroscopy. *Accounts chemical research* **51,** 2207–2214 (2018).

6. Salamanca Roldán, D. Medida de la sección eficaz de absorción de dos fotones correlacionados en átomos de cesio (2023).

7. Corona-Aquino, S. *et al.* Experimental study on the effects of photon-pair temporal correlations in entangled two-photon absorption. *arXiv preprint arXiv:2101.10987* (2021).

8. Caracas Núñez, M. S. Estudio teórico y experimental de la sección eficaz de la absorción de dos fotones en átomos de Cesio (2023).

9. Villabona-Monsalve, J. P., Calderón-Losada, O., Nuñez Portela, M. & Valencia, A. Entangled two photon absorption cross section on the 808 nm region for the common dyes zinc tetraphenylporphyrin and rhodamine b. *The J. Phys. Chem. A* **121,** 7869–7875 (2017).